ingegneria sismica
International Journal of Earthquake Engineering
Anno XLIII - Num. 2 - 2026

Predefined-Time Model-Free Sliding Mode Control for Permanent Magnet Synchronous Motor Speed Regulation Systems

Haoran Dai[1,*] *and Runmei Liu*[1]

[1] College of Electrical and Control Engineering, Liaoning Technical University, Huludao 125105, China

SUMMARY: *Aiming at the problems of parameter perturbation, external disturbance and poor robustness in permanent magnet synchronous motor (PMSM) speed regulation systems, this paper proposes a predefined-time model-free sliding mode control strategy combined with a predefined-time disturbance observer. Based on the ultra-local model, a predefined-time sliding mode surface and reaching law are designed to realize fast convergence independent of initial values. The observer accurately estimates lumped disturbances in real time for feedforward compensation. The analysis of Lyapunov stability has given a proof that convergence in predefined time is achieved. Both the simulation results and the hardware-in-the-loop experiment results have proven that the method put forward by us obviously decreases overshoot and settling time, strengthens the ability to reject disturbance, and thus has better performance than the traditional PI control in terms of dynamic response and robustness.*

KEYWORDS: *Permanent magnet synchronous motor; model-free sliding mode control; predefined-time sliding mode control; predefined-time observer*

1 Introduction

However, its actual working effect is frequently influenced by parameter uncertain conditions, outer load interferences, and own nonlinear properties, hence this requires strong and high-accuracy control methods. [1,2]. Because it has multiple variables, strong mutual coupling and very non-linear motion rules, the PMSM from its own nature is easy to be affected by outside interference and internal parameter uncertainty problems. Proportional-integral (PI) controlling still is the main strategy that has most uses for PMSM speed adjustment. But, its structure with fixed gain inherently has limitation on robustness, hence it causes large reduction in disturbance resisting ability and speed tracking precision when there exist big perturbations or parameter uncertainties[3].For solving these restrictions and getting promoted dynamic behavior together with strong interference resisting ability, a big number of advanced control methods have been deeply studied, including slip form control (SFC)[4], fuzzy logic control,[5] model prediction control (MPC)[6], and active interference rejection control (ADRC)[7]. In these methods, the sliding mode control (SMC) has got much attention in both academic circles and industrial fields, because it has natural anti-disturbance robustness and simple realization process[8,9]. Among the many research methods that have been worked out to promote closed-loop robustness, SMC has been already confirmed as a very effective nonlinear control method, especially for systems that have the features of strong nonlinearities and matched uncertainties.

*13188135115@163.com.
https://doi.org/10.65102/is2026997 Published: 30 April, 2026

SMC has been successfully utilized to promote the control performance of driving systems, mainly due to its inherent invariance characteristic which makes the sliding-phase dynamics not sensitive to matched uncertainties. Although conventional SMC has the natural firmness in resisting matched uncertainties, it still relies greatly on precise system models. In actual usage scenarios, though, unavoidable parameter changes and unknown integrated interferences often bring down the effect of control.For solving these existing shortcomings, this paper puts forward a model-free sliding mode control frame which has already been combined with a disturbance observer. The combination of no-model control and SMC effectively reduces dependence on exact motor parameter models, while the built-in disturbance observer actively makes up for total uncertainties, hence greatly improving the closed-loop anti-disturbance ability. For further lowering reliance on models,[10] recent research works have combined disturbance observation devices into model-free SMC frameworks. As an example, puts together a speed-loop sliding mode observer and a strengthened model-free SMC, thus [11] brings in an altered extended state observer (ESO) into an alike framework. Put together, these observer-increased model-no SMC methods – can effectively hold high tracking precision, and at the same time greatly promote closed-loop interference rejection ability.

The fast speed of convergence is one basic norm for evaluating performance when people design control systems. Although the conventional SMC which uses exponential reaching laws can guarantee robust tracking, its settling time still is intrinsically dependent on initial conditions.[12] Therefore, bigger initial state deviations without doubt bring about longer convergence time periods. For breaking through this restriction, the fixed-time convergence theory has been put forward, which can ensure that tracking errors can converge to a small neighbor area of the origin inside a uniformly bounded time length. Because the upper limit of the sedimentation time is a constant which is strictly not dependent on starting conditions, therefore observers and controllers based on fixed time have been widely researched at present[13,14].Even so, even though the fixed-time scheme’s settling time bound can be theoretically estimated beforehand, it still is implicitly connected with controller gains via a very high nonlinear relation, hence making it hard to directly give a needed convergence time length for special engineering demands. For the overcoming of this limitation, predefined-time control (PTC) has already arisen as one rigorous solution. Its special distinguishing character is that the convergence time limit may be clearly given as a direct adjustment parameter, which remains strictly not dependent on starting conditions and other control gains, hence therefore enabling truly user-given convergence [15]. Based on this frame, [16] puts PTC and sliding mode control together to make a predefined-time sliding mode controller, which together mixes robust disturbance resistance with clearly ensured transient performance.Extending this paradigm, [17] integrates an extended state observer (ESO) with predefined-time SMC to enhance disturbance attenuation, while rigorously preserving the explicitly prescribed convergence bound.

This study proposes a predefined-time model-free sliding mode control (PT-MF-SMC) scheme for PMSM drives. A predefined-time sliding mode controller is designed to guarantee fast convergence within a user-settled time. A predefined-time sliding mode disturbance observer is constructed to estimate and compensate uncertainties. Stability is strictly proved via Lyapunov theory. Simulation and experimental results validate that the proposed method achieves superior speed tracking, stronger disturbance rejection and better robustness under parameter variations and load impacts.

2 Mathematical Model of PMSM

In the synchronous rotation d-q reference coordinate frame, the idealized speed-loop dynamic equation of the surface-mounted permanent magnet synchronous motor (SPMSM) can be written as:

$$\dot{\omega} = (1.5 n_p \psi_f i_q - B_f \omega - T_L) / J \tag{1}$$

where i_q denotes the q-axis stator current, T_L is the load torque, B_f represents the viscous friction coefficient, ψ_f is the permanent magnet flux linkage, ω denotes the mechanical rotor speed, n_p is the number of pole pairs, and J stands for the total moment of inertia.

However, in practical drive applications, the system dynamics are inevitably subject to parameter variations, unmodeled nonlinearities, and external disturbances. To comprehensively account for these effects, the PMSM speed dynamics can be reformulated as:

$$\dot{\omega} = (1.5 n_p \psi_{f0} i_q - B_{f0} \omega - f) / J_0 \tag{2}$$

$$f = \Delta J \omega^{'} - 1.5 n_p \Delta \psi_f i_q + \Delta B_f \omega + T_L \tag{3}$$

where B_{f0}, ψ_{f0}, and J_0 denote the nominal values of the viscous friction coefficient, permanent magnet flux linkage, and total moment of inertia, respectively; where ΔB_f, $\Delta \psi_f$, and ΔJ denote the parametric deviations of the viscous friction coefficient, permanent magnet flux linkage, and moment of inertia, respectively; and f represents the lumped disturbance acting on the speed loop.

In the synchronous rotating d-q reference frame, the PMSM speed dynamics are reformulated via an ultra-local model to circumvent reliance on precise plant parameters. This control-oriented representation decouples the known input channel from aggregated unknown dynamics, and is expressed as:

$$i_q^* = \frac{-F - \beta \omega + \dot{\omega}^* + u_c}{\alpha} \tag{4}$$

Consequently, the speed-loop dynamics are decoupled into a known linear control channel and an aggregated nonlinear uncertainty term. In (4), α denotes the designable pseudo-control gain, while F represents the lumped unknown dynamics to be estimated. Specifically, F encapsulates all parametric uncertainties, unmodeled nonlinearities, and external load disturbances acting on the PMSM speed loop.

This model effectively avoids dependence on accurate motor parameters and provides a concise control-oriented expression for the design of model-free controllers.

3 Predefined-Time Model-Free Sliding Mode Control Design

3.1 Controller Design

In this segment, a speed tracking control strategy for permanent magnet synchronous motor

(PMSM) drives is formulated within the framework of the proposed predefined - time model - free sliding mode control (PT - MF - SMC). In contrast to traditional sliding mode control (SMC), the designed controller ensures that the system states reach the sliding manifold and the tracking error converges to a small vicinity of the origin within a precisely predefined time limit, regardless of the initial conditions. This design efficiently expedites the transient response, improves the closed - loop dynamic performance, and surmounts the initial - state dependency characteristic of traditional sliding mode approaches. By integrating the predefined - time convergence concept into the integral sliding manifold, the switching surface is established as follows:

$$s = e + \int_o^t (c_1 \mathrm{sign}(e) |e|^{1+\lambda_1} + c_2 \mathrm{sign}(e) |e|^{1-\lambda_1} + c_3 \mathrm{sign}(e)) \mathrm{d}\tau \tag{5}$$

where $c_1 = \frac{\pi}{\lambda_1 T_{c_1}} \left(\frac{1}{2}\right)^{1+\frac{\lambda_1}{2}}$, $c_2 = \frac{\pi}{\lambda_1 T_{c_1}} \left(\frac{1}{2}\right)^{1-\frac{\lambda_1}{2}}$, and $c_3 > 0$ denote the tunable design parameters; T_{c_1} represents the predefined settling time bound during the sliding phase; $\lambda_1 \in (0,1)$ is an additional control gain; and e stands for the speed tracking error.

To guarantee that the sliding variable converges to zero within the predefined settling time, the reaching law is designed as:

$$\dot{s} = -c_4 \mathrm{sign}(s) |s_1|^{1+\gamma_1} - c_5 \mathrm{sign}(s) |s|^{1-\gamma_1} - c_6 \mathrm{sign}(s) \tag{6}$$

where $c_4 = \frac{\pi}{\gamma_1 T_{c_2}} \left(\frac{1}{2}\right)^{1+\frac{\gamma_1}{2}}, c_5 = \frac{\pi}{\gamma_1 T_{c_2}} \left(\frac{1}{2}\right)^{1-\frac{\gamma_1}{2}}$ and $c_6 > 0$ denote the tunable design parameters; T_{c_2} represents the predefined upper bound for the reaching phase duration to the sliding manifold; $\gamma_1 \in (0,1)$ is an additional control gain; and s stands for the sliding manifold variable.

By incorporating the sliding manifold (5) and the reaching law (6) into the speed - loop ultra - local model, the predefined - time model - free sliding mode speed controller is formulated as follows:

$$\begin{aligned} i_q^* = \; & \frac{1}{\alpha} (\dot{\omega}^* - \beta\omega - F + \\ & c_1 \mathrm{sign}(e) |e|^{1+\lambda_1} + c_2 \mathrm{sign}(e) |e|^{1-\lambda_1} + c_3 \mathrm{sign}(e) + \\ & c_4 \mathrm{sign}(s_1) |s_1|^{1+\gamma_1} + c_5 \mathrm{sign}(s_1) |s|^{1-\gamma_1} + c_6 \mathrm{sign}(s_1)) \end{aligned} \tag{7}$$

The crafted control rule guarantees that the speed tracking deviation converges to the zero point within the pre - set time, attaining a rapid and precise dynamic reaction.

3.2 Stability and Convergence Analysis

Lemma 1 [18]: Suppose there is a potential Lyapunov function V for which the time - derivative of V along the system's trajectories adheres to the following condition:

$$\dot{V} \le -\frac{\pi}{\lambda T_c} \left(V^{1+\frac{\lambda}{2}} + V^{1-\frac{\lambda}{2}} \right) \tag{8}$$

where $\lambda \in (0,1)$, and T_c are positive constants. Under this condition, the closed-loop system is predefined-time stable, the origin constitutes a predefined-time stable equilibrium point, and the actual settling time is strictly upper-bounded by the explicitly prescribed constant T_c, independent of initial conditions.

To demonstrate the convergence characteristic of the proposed controller within a pre - determined time, the subsequent candidate for the Lyapunov function is formulated:

$$V_1 = \frac{1}{2}s^2 \tag{9}$$

When differentiating the Lyapunov candidate presented in equation (9) with respect to time as it follows the closed - loop trajectories, the following result is obtained:

$$\begin{aligned}
\dot{V}_1 &= s\dot{s} \\
&= s\left(-c_4\text{sign}(s)\,|s|^{1+\gamma_1} - c_5\text{sign}(s)\,|s|^{1-\gamma_1} - c_6\text{sign}(s)\right) \\
&= -c_4\,|s|^{2-\gamma_1} - c_5\,|s|^{2-\gamma_1} - c_6\,|s| \\
&\le -\frac{\pi}{\gamma_1 T_{c_2}}\left(\frac{1}{2}\right)^{1+\frac{\gamma_1}{2}}|s|^{2+\gamma_1} - \frac{\pi}{\gamma_1 T_{c_2}}\left(\frac{1}{2}\right)^{1-\frac{\gamma_1}{2}}|s|^{2-\gamma_1} \\
&= -\frac{\pi}{T_{c_2}\gamma_1}(V_1^{1+\frac{\gamma_1}{2}} + V_1^{1-\frac{\gamma_1}{2}})
\end{aligned} \tag{10}$$

By comparing the differential inequality (10) with the condition established in Lemma 1, it is evident that the proposed control scheme satisfies the predefined-time stability criterion. Consequently, the system trajectories are guaranteed to reach the sliding manifold within the explicitly prescribed time bound T_{c_2}, strictly independent of initial conditions.

Once the system's trajectories arrive at the sliding manifold, the dynamics of the closed - loop are restricted to develop precisely along the surface. In the case of the ideal sliding condition where and , the dynamics of the reduced - order tracking error can be obtained as follows:

$$\dot{e} = -c_1\text{sign}(e)\,|e|^{1+\lambda_1} - c_2\text{sign}(e)\,|e|^{1-\lambda_1} - c_3\text{sign}(e) \tag{11}$$

To achieve the convergence of the tracking error on the sliding manifold within a pre - determined time, the following potential Lyapunov function is built [19, 20].

$$V = \frac{1}{2}e^2 \tag{12}$$

Differentiating the Lyapunov function candidate (12) with respect to time along the reduced-order error dynamics yields:

$$\begin{aligned}\dot{V}_2 &= e\dot{e}\\ &= e(-c_1\mathrm{sign}(e)\,|e|^{1+\lambda_1} - c_2\mathrm{sign}(e)\,|e|^{1-\lambda_1} - c_3\mathrm{sign}(e))\\ &= -c_1\,|e|^{2-\lambda_1} - c_2\,|e|^{2-\lambda_1} - c_3\,|e|\\ &\le -\frac{\pi}{\lambda_1 T_{c_1}}\left(\frac{1}{2}\right)^{1+\frac{\lambda_1}{2}}|e|^{2-\lambda_1} - \frac{\pi}{\lambda_1 T_{c_1}}\left(\frac{1}{2}\right)^{1-\frac{\lambda_1}{2}}|e|^{2-\lambda_1}\\ &= -\frac{\pi}{T_{c_1}\lambda_1}(V_2^{\,1+\frac{\lambda_1}{2}} + V_2^{\,1-\frac{\lambda_1}{2}})\end{aligned} \tag{13}$$

Consequently, the derived Lyapunov inequality strictly aligns with the condition stipulated in Lemma 1. This guarantees that the tracking error e evolves on the sliding manifold and converges to a small neighborhood of the origin within the explicitly prescribed time bound T_{c_1} ,strictly independent of initial conditions.

The Lyapunov assessment validates that the closed - loop system exhibits global predefined - time stability. This stability guarantees dependability and convergence characteristics across a wide range of operating circumstances.

4 Predefined-Time Sliding Mode Observer Design

In this section, the lumped uncertainty is augmented as an extended state variable. Accordingly, a predefined-time sliding mode disturbance observer (PT-SMDO) is designed to achieve accurate real-time estimation of F . The augmented ultra-local model for the PMSM speed loop is formulated as [21-24]:

$$\begin{cases}\dfrac{\mathrm{d}\omega}{\mathrm{d}t} = \alpha i_{\mathrm{q}} + \beta\omega + F\\ \dfrac{\mathrm{d}F}{\mathrm{d}t} = \xi(t)\end{cases} \tag{14}$$

A predefined - time sliding mode disturbance observer (PT - SMDO) for the speed loop is formulated as follows:

$$\begin{cases}\dfrac{\mathrm{d}\hat{\omega}}{\mathrm{d}t} = \alpha i_{\mathrm{q}} + \beta\hat{\omega} + \hat{F} + u_{\mathrm{smo}}\\ \dfrac{\mathrm{d}\hat{F}}{\mathrm{d}t} = l\cdot u_{\mathrm{smo}}\end{cases} \tag{15}$$

where $\hat{\omega}$ denotes the estimated mechanical speed, $\hat{F}$ represents the real-time estimate of the lumped uncertainty, $\mathrm{d}\hat{F}/\mathrm{d}t$ stands for its time derivative, u_{smo} is the predefined-time sliding mode injection function to be designed, and $l_1 > 0$ denote the observer gains.

Defining the estimation errors as $e_\omega = \hat{\omega} - \omega$ and $e_{\mathrm{dis}} = \hat{F} - F$ the error dynamics are derived as:

$$\begin{cases} \dot{e}_\omega = \beta e_\omega + e_{\text{dis}} + u_{\text{smo}} \\ \dot{e}_{\text{dis}} = l \cdot u_{\text{smo}} - \xi(t) \end{cases} \tag{16}$$

where $e_\omega = \hat{\omega} - \omega$ denotes the speed estimation error, and $e_{\text{dis}} = \hat{F} - F$ represents the estimation error of the lumped uncertainty.

To enforce predefined-time convergence of the estimation errors, the nonlinear reaching law is designed as:

$$\dot{s}_\omega = -c_7 \text{sign}(s_\omega) |\, s_\omega \,|^{1+\rho_1} - c_8 \text{sign}(s_\omega) |\, s_\omega \,|^{1-\rho_1} - c_9 \text{sign}(s_\omega) \tag{17}$$

where $c_7 = \dfrac{\pi}{\rho_1 T_{c_3}} \left(\frac{1}{2}\right)^{1+\frac{\rho_1}{2}}$, $c_8 = \dfrac{\pi}{\rho_1 T_{c_3}} \left(\frac{1}{2}\right)^{1-\frac{\rho_1}{2}}$, and $c_9 > 0$ denote the tunable design parameters, and $\rho_1 \in (0,1)$ represents an additional observer gain.

By defining the sliding manifold $s_\omega = e_\omega$ and substituting (16) into (17), the term e_{dis} is treated as a bounded perturbation acting on u_{smo} .Consequently, the explicit expression for the predefined-time sliding mode injection function is derived as:

$$u_{\text{smo}} = -\beta e_\omega - c_7 \text{sign}(e_\omega) |\, e_\omega \,|^{1+\rho_1} - c_8 \text{sign}(e_\omega) |\, e_\omega \,|^{1-\rho_1} - c_9 \text{sign}(e_\omega) \tag{18}$$

By constructing the sliding manifold $s_\omega = e_\omega$ and employing the predefined-time reaching law (17), the design parameter $c_9 \geq |\, e_{\text{dis}} \,|$ are appropriately tuned to guarantee that the state error defined in (18) converges to a small neighborhood of the origin within the explicitly prescribed time bound, strictly independent of initial conditions.

To rigorously establish the stability of the proposed disturbance observer, the following Lyapunov function candidate is constructed:

$$V_3 = \frac{1}{2} s_\omega^2 \tag{19}$$

Differentiating the Lyapunov candidate (18) with respect to time along the estimation error dynamics yields:

$$\begin{aligned} \dot{V}_3 &= e_\omega \dot{e}_\omega \\ &= e_\omega (\beta e_\omega + e_{\text{dis}} + u_{\text{smo}}) \\ &= e_\omega (e_{\text{dis}} - c_7 \text{sign}(e_\omega) |\, e_\omega \,|^{1+\rho_1} - c_8 \text{sign}(e_\omega) |\, e_\omega \,|^{1-\rho_1} - c_9 \text{sign}(e_\omega)) \\ &= |\, e_\omega \,| (|\, e_{\text{dis}} \,| - c_9) - c_7 |\, e_\omega \,|^{2+\rho_1} - c_8 |\, e_\omega \,|^{2-\rho_1} \end{aligned} \tag{20}$$

To guarantee $\dot{V}_3 \leq -\dfrac{\pi}{T_{c_2} \rho_1} (V^{1+\frac{\rho_1}{2}} + V^{1-\frac{\rho_1}{2}})$, the observer design parameters c_9 must satisfy the following conditions:

$$c_9 \geq |\, e_{\text{dis}} \,| \tag{21}$$

By appropriately tuning the observer parameters c_9, the derived Lyapunov inequality $\dot{V}_3 \le -\frac{\pi}{T_{c_3}\rho_1}(V^{1+\frac{\rho_1}{2}} + V^{1-\frac{\rho_1}{2}})$ strictly aligns with the condition stipulated in Lemma 1. Consequently, the estimation error trajectories are guaranteed to reach the sliding manifold within the explicitly prescribed time bound T_{c_3}, strictly independent of initial estimation conditions.

Synthesizing the ultra-local model dynamics, the predefined-time reaching law, and the real-time disturbance compensation, the complete control input is formulated as:

$$\begin{aligned} i_q^* = \ & \frac{1}{\alpha}(\dot{\omega}_m^* - \beta\omega_m - \hat{F} + \\ & c_1\mathrm{sign}(e)|e|^{1+\lambda_1} + c_2\mathrm{sign}(e)|e|^{1-\lambda_1} + c_3\mathrm{sign}(e) + \\ & c_4\mathrm{sign}(s)|s|^{1+\gamma_1} + c_5\mathrm{sign}(s)|s|^{1-\gamma_1} + c_6\mathrm{sign}(s)) \end{aligned} \tag{22}$$

To mitigate chattering induced by the discontinuous $\mathrm{sign}(\cdot)$ function in sliding mode control, the hyperbolic $\tanh(\cdot)$ function is employed as a continuous approximation.

The proposed predefined-time observer can quickly and accurately estimate lumped disturbances, which provides reliable compensation for the controller to suppress disturbances.

5 Simulation and Experimental Validation

To verify the efficacy and practicality of the proposed control strategy, a simulation model for the PMSM vector control system is constructed within the MATLAB/Simulink environment, as shown in Figure 1. The specific motor parameters employed for the simulation are presented in Table 1.

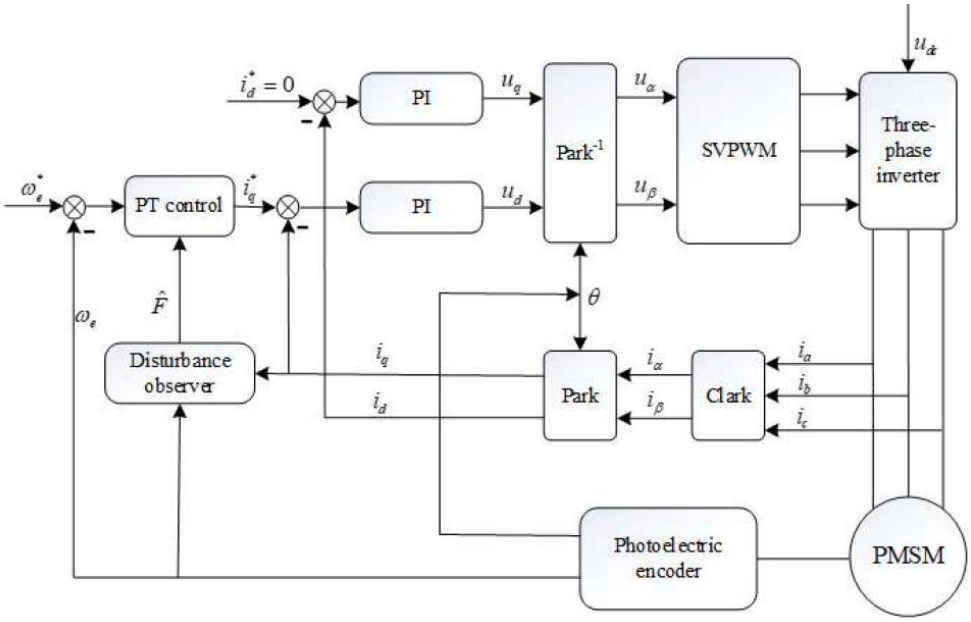

Figure 1: Block diagram of the proposed predefined-time model-free sliding mode control (PT-MF-SMC) framework.

In our experimental setup, we utilize a surface-mounted permanent magnet synchronous motor (SPMSM). The standard specifications of the motor under test are summarized in Table 1.

Table 1: Nominal Parameters of the PMSM

Nominal parameters	Value
Stator resistance $R_s(\Omega)$	0.346
d- and q-axis inductances L(H)	0.0078
Viscous friction coefficient $B(\mathrm{N\cdot m\cdot s})$	0.005
Moment of inertia $J(\mathrm{kg\cdot m^2})$	0.089
Permanent magnet flux linkage $\psi_f(\mathrm{V\cdot s})$	0.51825
Number of pole pairs p_n	2
Rated power (kW)	10
Rated voltage (V)	260
Rated speed (r/min)	1500

To comprehensively evaluate the proposed approach, the simulation benchmarks the speed controller designed with the conventional PI strategy against the proposed PT-MF-SMC scheme. In this work, the predefined-time parameters T_{c1}, T_{c2}, and T_{c3} are set to 0.2s, 0.2s, and 0.4s, respectively [25-28].

The corresponding controller parameter quantities are gathered in Table 2.

Table 2: Controller Parameters for the Comparative Schemes

Experimental	Tuning parameters
PI control	$k_p = 0.527, k_i = 8.106$
PT control	α =19.422, β =-0.051, c_1 =7.920, c_2 =8.841, c_3 =52.61, c_4 =19.332, c_5 =24.837, c_6 =55.56, c_7 =9.427, c_8 =12.180, c_9 =11.859, λ_1 =0.362, γ_1 =0.358, ρ_1 =0.366, l =0.507

6 Dynamic Loading and Unloading Test

The motor experiment is set to have a no-load starting velocity of 400 r/min. One load torque of 10 N·m is suddenly added when t equals 1s and is removed when t equals 2s. The traditional PI controller possesses evident speed overshoot and comparatively slow settling velocity, with big speed deviation and long recovery duration when load changes occur suddenly. It also generates very serious d-q axis current undulations and clear current wave motions. By way of comparison, the put-forward PT-MF-SMC method greatly decreases speed overshoot, cuts short settling and recovery time, and effectively holds down current ripples. It can keep smooth electric current shape graphs and smaller rotate speed change vibration under load instant change situations. The experiment results verify this put-forward control method possesses better dynamic working performance, stronger anti-disturbance capability and more excellent robustness with respect to unexpected load changes.

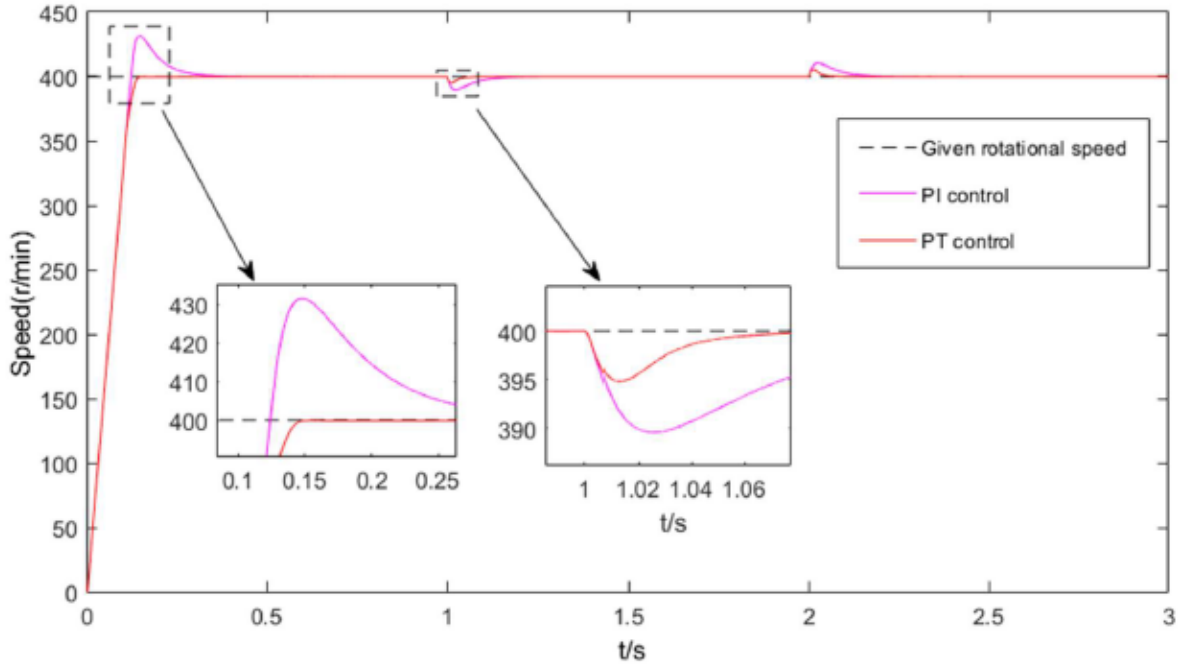

Figure 2: Loading and Unloading Speed Comparison Curve

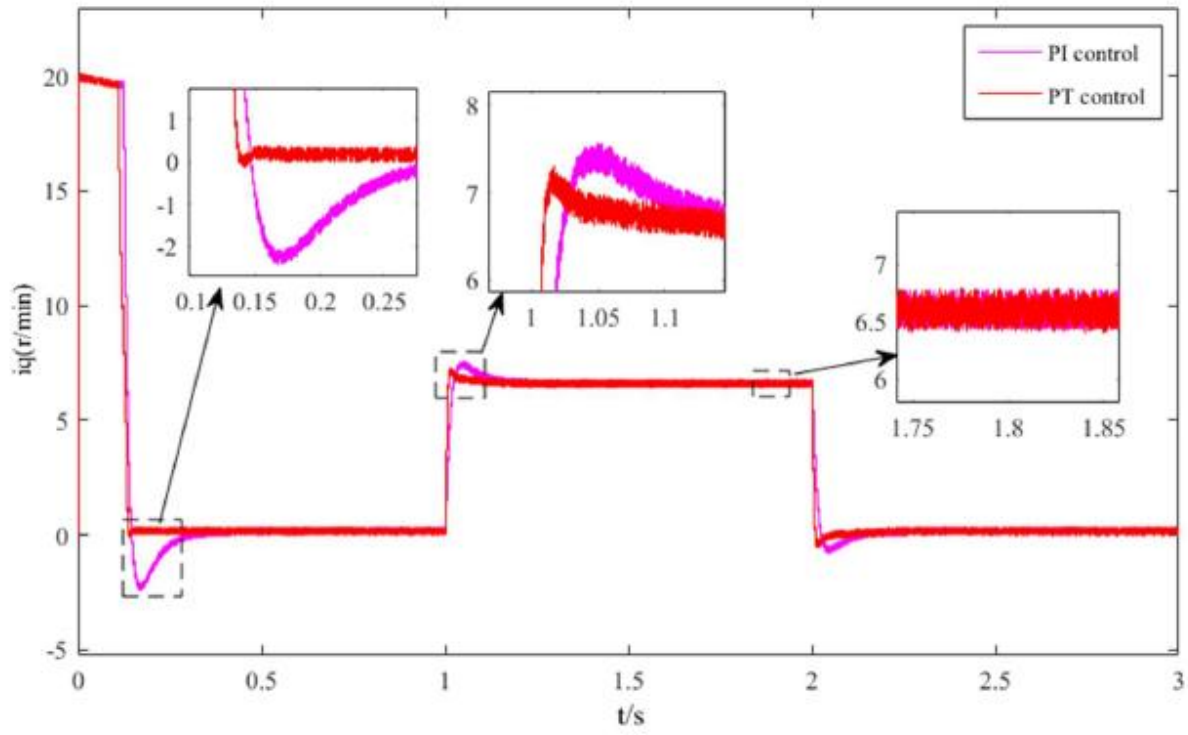

Figure 3: iq (q-axis) Current Comparison Curve during Loading and Unloading

7 Speed Reversal and Ramp Tracking Tests

Two dynamic speed following situations are set up for assessing transient property. In the acceleration and deceleration experiment, the electric machine begins to move at 300 r/min, the reference rotating speed is commanded to reach 500 r/min at the moment t = 1s, and therefore

it is sent back to 300 r/min at the moment t = 2s. Within the speed reversal experiment, the electric motor at the beginning works at 200 r/min, and the speed instruction is suddenly reversed to -200r/min when t equals 1.5s. The comparison of tracking responses under these two working conditions is demonstrated in Figure 4 and 5, respectively.

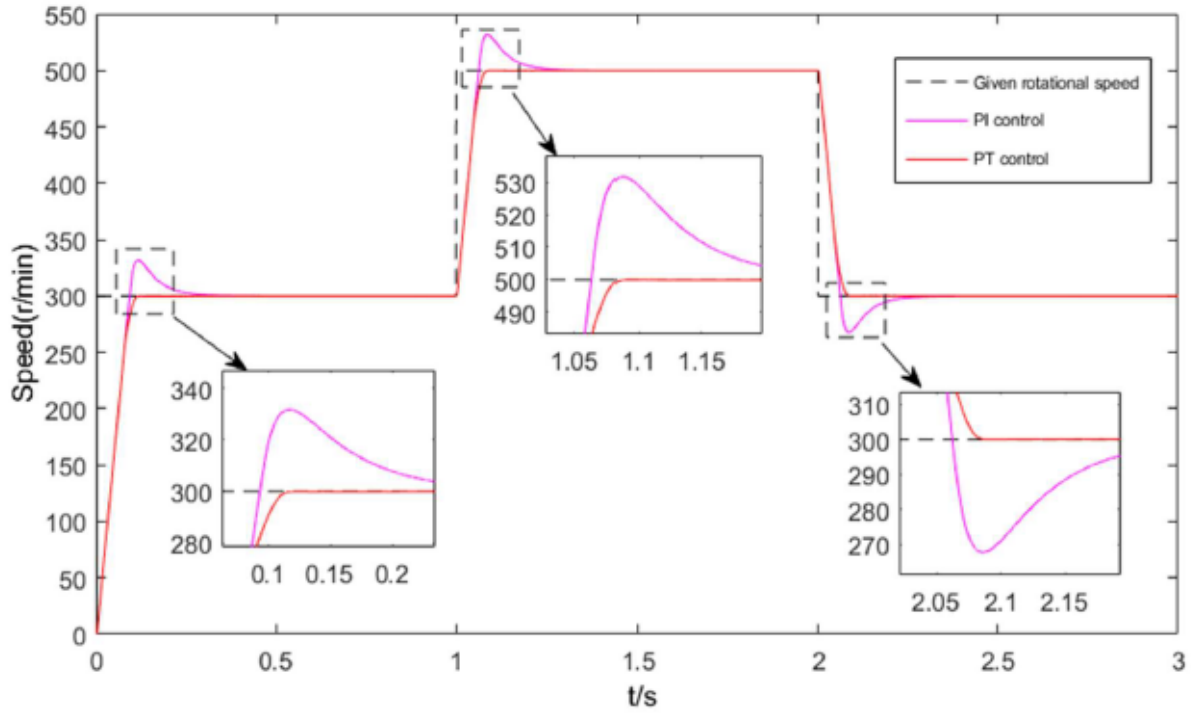

Figure 4: Comparative speed tracking response during acceleration and deceleration transients.

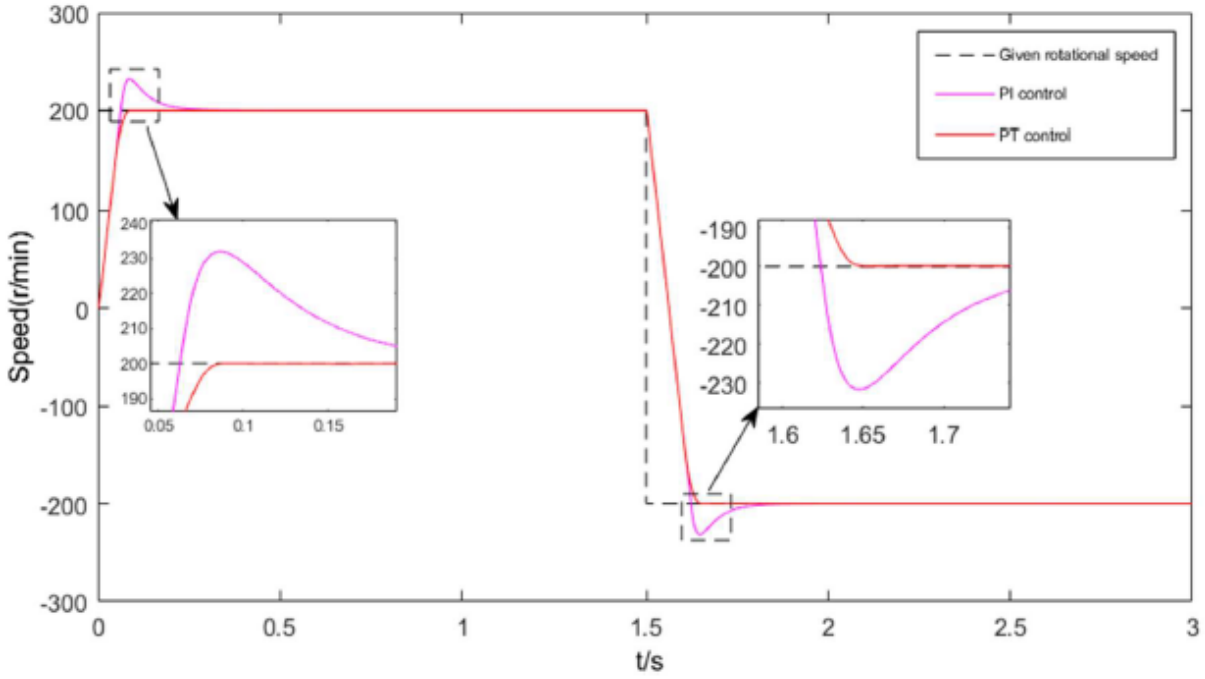

Figure 5: Comparative speed tracking response during bidirectional speed reversal.

Through analyzing Figure 4 and Figure 5 we can know that the traditional PI controller has obvious overshoot and relatively large speed undulations in the processes of both acceleration, deceleration and speed reversal transient processes. By comparison, the put forward PT-MF-SMC keeps more smooth speed changes with greatly decreased overshoot and very small vibrations. These comparison results have clearly proven that the dynamic performance of the scheme we put forward is better. In addition, the simulation results have proven that, under various working situations, the put-forward method obviously has better performance than the traditional PI baseline, providing strengthened disturbance resistance, reduced speed difference, quicker transient reaction, and effectively decreased current waves, hence it proves its good robustness and engineering feasibility [29-32].

8 Experimental Validation

For confirming that the actual effect and the real-time possibility of the scheme we put forward is correct, all-round experiments are carried out on a hardware-in-the-loop (HIL) test platform. One photograph that shows the integrated motor drive and dynamometer loading platform is put in Figure 6. The experiment arrangement mainly is composed by a PWM voltage resource inverter, a motor drive and mechanical load system, a National Instruments (NI) real-time control device, a host PC for real-time watch and data collect, and related power distribution and signal adjust circuits.

Figure 6: Photograph of the integrated motor drive and dynamometer loading testbed.

9 Hardware Validation Under Sudden Load Torque Perturbation

In the hardware experiment, the motor initial no-load speed is set at 400 r/min by us. After the stable running work, 10 N·m load torque suddenly is exerted and then is taken away. The traditional PI controller possesses long time for setting, big speed fall, slow speed restoration, and serious q-axis current wave fluctuations when load switches. The PT-MF-SMC which we

put forward greatly shortens the settling time, sharply cuts down speed fluctuation, and therefore realizes fast speed recovery. It also has effective suppression function on current ripples and chattering. The hardware experiment outcomes prove that the method put forward gives quicker dynamic response, bigger anti-interference ability and more good robustness. It holds pre-given-time convergence property toward sensor noise, inverter dead-time and mechanical time lags in real practice.

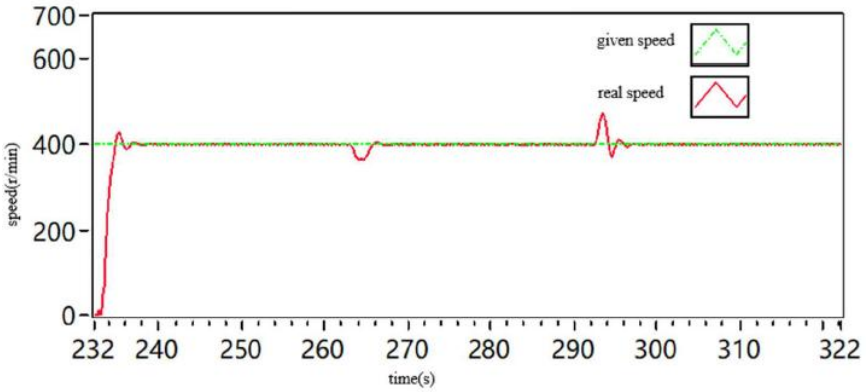

Figure 7: Experimental speed tracking response of the conventional PI controller under dynamic loading and unloading.

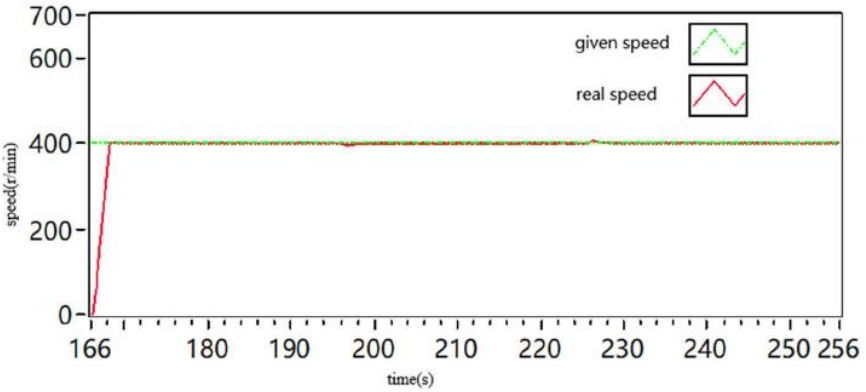

Figure 8: Experimental speed tracking response of the conventional PI controller under dynamic loading and unloading.

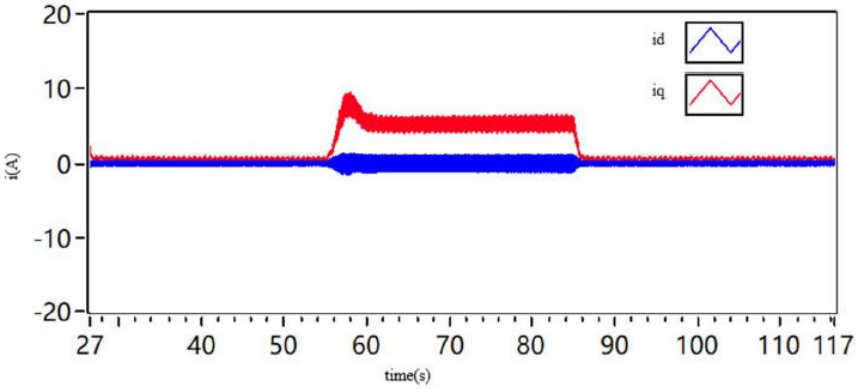

Figure 9: Experimental d- and q-axis current waveforms of the conventional PI controller under dynamic loading.

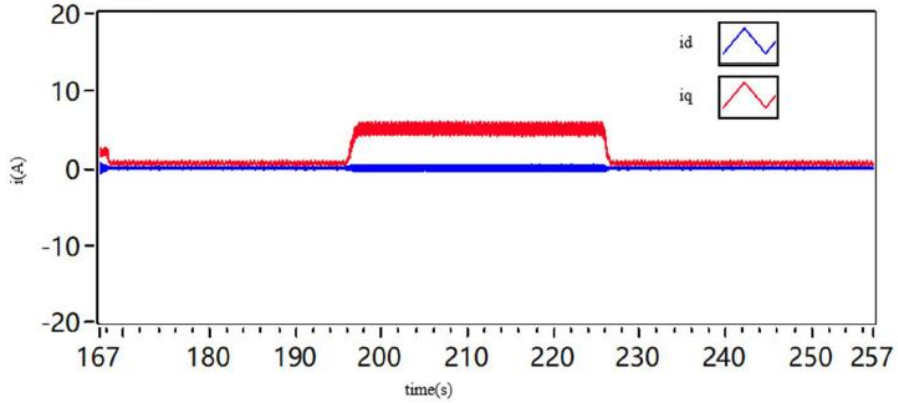

Figure 10: Experimental d- and q-axis current waveforms of the conventional PI controller under dynamic loading.

10 Hardware Validation Under Dynamic Speed Tracking and Reversal

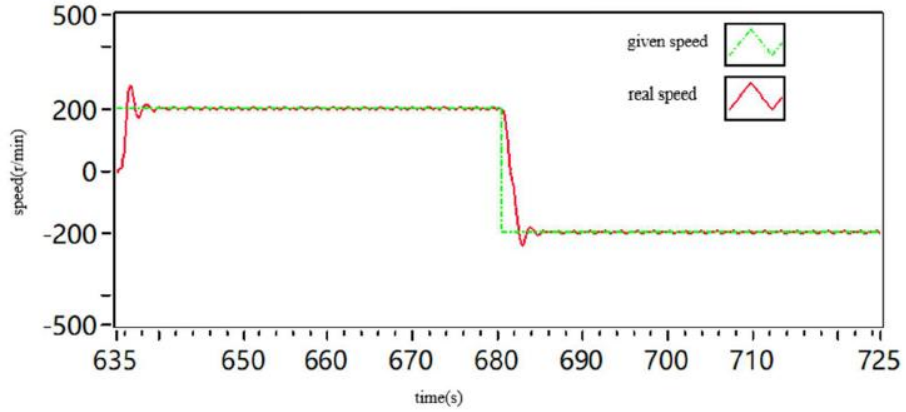

Figure 11: Experimental speed tracking response of the conventional PI controller during bidirectional speed reversal

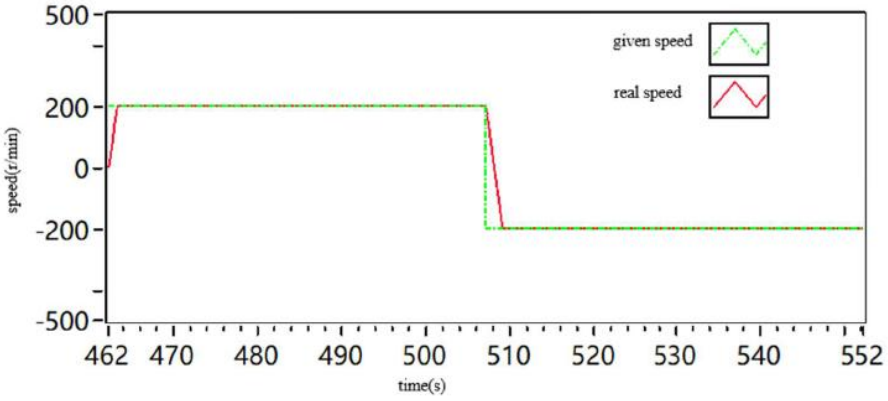

Figure 12: Experimental speed tracking response of the conventional PI controller during bidirectional speed reversal.

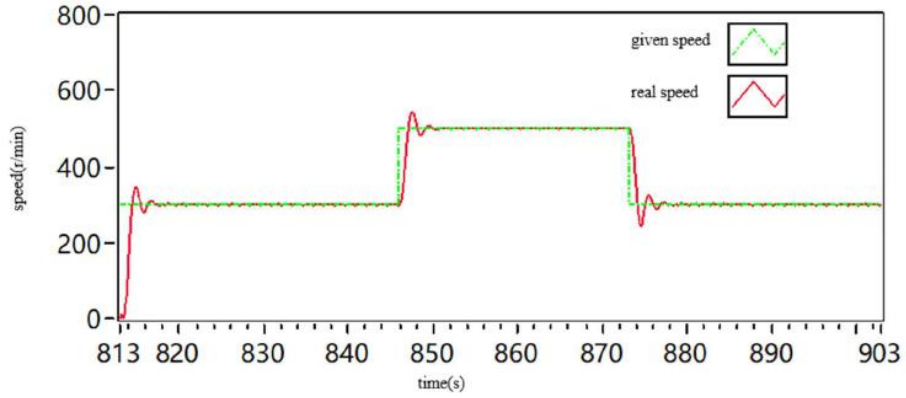

Figure 13: Experimental speed tracking response of the conventional PI controller during acceleration and deceleration transients.

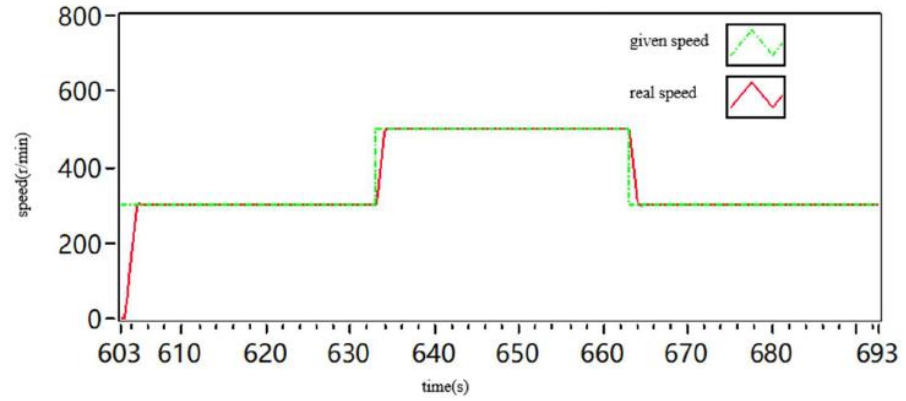

Figure 14: Experimental speed tracking response of the conventional PI controller during acceleration and deceleration transients.

The dynamic experimental tests are conducted under two representative operating trajectories. In the acceleration/deceleration test, the motor initially operates at 300r/min. Upon reaching steady state, the reference speed is commanded to 500r/min, and after stabilization, it is returned to 300r/min. For the bidirectional reversal test, the motor runs at +200r/min before the command is abruptly switched to -200r/min. The comparative experiment responses under these two situation are given in Figure 11, 12, 13, and 14. Through observation, the PT-MF-SMC put forward by us obtains extremely smooth speed change processes with extremely tiny overshoot in both ramp tracking and zero-crossing reversal work. By comparison, the traditional PI controller (Scheme 1) shows obvious speed vibration waves and obvious overshoot when the reference value changes.

11 Conclusions

This article puts forward a predefined-time non-model sliding mode control approach for PMSM speed adjusting systems. The controller which we have designed and the observer which we constructed can reach the pre-set time convergence, and possess the strong ability of disturbance rejection. Simulation and hardware experiments make confirmation that the strategy which we put forward can decrease overshoot, shorten the time that system reaches stable state, restrain speed fluctuation when load has disturbance, hence hence significantly promote the robustness and dynamic performance of system.

CRediT authorship contribution statement

Haoran Dai: Writing – review & editing, Writing – original draft, Validation, Software, Funding acquisition, Data curation. **Runmei Liu**: Writing – review & editing, Software, Methodology, Formal analysis, Data curation, Conceptualization.

Declaration of competing interest

The authors declare that they have no known competing financial interests or personal relationships that could have appeared to influence the work reported in this paper.

Acknowledgements

The authors gratefully acknowledge the support and guidance received from colleagues and experts in the field of coal mine safety and gas extraction technology. Their insightful comments and suggestions have significantly contributed to the improvement of this work.

This research was conducted without any external financial support.

Data availability

Data will be made available on request.

References

[1] Rafaq M S, Midgley W, Steffen T. A review of the state of the art of torque ripple minimization techniques for permanent magnet synchronous motors[J]. IEEE Transactions on Industrial Informatics, 2023, 20(1): 1019-1031.

[2] Cai W, Wu X, Zhou M, et al. Review and development of electric motor systems and electric powertrains for new energy vehicles[J]. Automotive Innovation, 2021, 4(1): 3-22.

[3] Singh A K, Raja R, Sebastian T, et al. Limitations of the PI control with respect to parameter variation in PMSM motor drive systems[C]//2019 IEEE International Electric Machines & Drives Conference (IEMDC). IEEE, 2019: 1688-1693.

[4] Gao P, Zhao C, Pan H, et al. A model-free fractional-order composite control strategy for high-precision positioning of permanent magnet synchronous motor[J]. Fractal and Fractional, 2025, 9(3): 161.

[5] Guo L, Zhang X, Zheng C, et al. A new fuzzy sliding mode control method for permanent magnet synchronous motor servo system based on optimization of fuzzy rules[J]. IEEJ Transactions on Electrical and Electronic Engineering, 2022, 17(12): 1748-1754.

[6] An X, Liu G, Chen Q, et al. Adjustable model predictive control for IPMSM drives based on online stator inductance identification[J]. IEEE Transactions on Industrial Electronics, 2021, 69(4): 3368-3381.

[7] Liu X, Zhang G, Shi Z. Improved current control for PMSM via an active disturbance

rejection controller[J]. European Journal of Control, 2024, 78: 101005.

[8] Guo X, Huang S, Lu K, et al. A fast sliding mode speed controller for PMSM based on new compound reaching law with improved sliding mode observer[J]. IEEE Transactions on Transportation Electrification, 2022, 9(2): 2955-2968.

[9] Cao S, Liu J, Yi Y. Non-singular terminal sliding mode adaptive control of permanent magnet synchronous motor based on a disturbance observer[J]. The Journal of Engineering, 2019, 2019(15): 629-634.

[10] Gao P, Zhang G, Lv X. Model-free control using improved smoothing extended state observer and super-twisting nonlinear sliding mode control for PMSM drives[J]. Energies, 2021, 14(4): 922.

[11] Shi Y, Mei K. Adaptive nonsingular terminal sliding mode controller for PMSM drive system using modified extended state observer[J]. Mathematical biosciences and engineering: MBE, 2023, 20(10): 18774-18791.

[12] Cooperative control of multi-agent systems: Theory and applications[J]. 2017.

[13] Hong H, Yu C, Yu W. Adaptive fixed-time control for attitude consensus of disturbed multi-spacecraft systems with directed topologies[J]. IEEE Transactions on Network Science and Engineering, 2022, 9(3): 1451-1461.

[14] Liu J, Li R, Zheng J, et al. Novel flexible fixed-time stability theorem and its application to sliding mode control nonlinear systems[J]. Review of Scientific Instruments, 2024, 95(8).

[15] Song Y, Ye H, Lewis F L. Prescribed-time control and its latest developments[J]. IEEE Transactions on Systems, Man, and Cybernetics: Systems, 2023, 53(7): 4102-4116.

[16] Yue X, Zhang H, Ma J. Predefined-time safe cooperative control for multiagent systems with privacy preservation and unknown disturbances[J]. IEEE Transactions on Cybernetics, 2025.

[17] Xu C, Wu B, Zhang Y. Distributed prescribed-time attitude cooperative control for multiple spacecraft[J]. Aerospace science and technology, 2021, 113: 106699.

[18] Zhang M, Zang H, Bai L. A new predefined-time sliding mode control scheme for synchronizing chaotic systems[J]. Chaos, Solitons & Fractals, 2022, 164: 112745.

[19] He Y, Xiao L, Wang Z, et al. A fuzzy neural network approach to adaptive robust nonsingular sliding mode control for predefined-time tracking of a quadrotor[J]. IEEE Transactions on Fuzzy Systems, 2024, 32(12): 6775-6788.

[20] Ni J, Liu L, Tang Y, et al. Predefined-time consensus tracking of second-order multiagent systems[J]. IEEE Transactions on Systems, Man, and Cybernetics: Systems, 2019, 51(4): 2550-2560.

[21] Yang X, Yan B, Han Y, et al. Nonsingular Generalized Adjustable Predefined-Time Sliding Mode Controllers with Adaptive Predefined-Time Observers for Nonlinear

Dynamical Systems[J]. IEEE Transactions on Automation Science and Engineering, 2026.

[22] Huang S, Xu Z, Xiong L, et al. Predefined-time observer-based sliding mode control for fast frequency support in heterogeneous power system through grid-forming converter[J]. IEEE Transactions on Power Systems, 2025.

[23] Chen J, Chen Z, Zhang H, et al. Predefined-time observer-based nonsingular sliding-mode control for spacecraft attitude stabilization[J]. IEEE Transactions on Circuits and Systems II: Express Briefs, 2023, 71(3): 1291-1295.

[24] Cai G, Shang Y, Xiao Y, et al. Predefined-time sliding mode control with neural network observer for hypersonic morphing vehicles[J]. IEEE Transactions on Aerospace and Electronic Systems, 2025.

[25] Lai C K, Tsao Y T, Tsai C C. Modeling, analysis, and realization of permanent magnet synchronous motor current vector control by MATLAB/simulink and FPGA[J]. Machines, 2017, 5(4): 26.

[26] Boby K, Kottalil A M, Ananthamoorthy N P. Mathematical modelling of pmsm vector control system based on SVPWM with pi controller using Matlab[J]. International Journal of Advanced Research in Electrical, Electronics and Instrumentation Engineering, 2013, 2(1).

[27] Adeoye A O M, Oladapo B I, Adekunle A A, et al. Design, simulation and implementation of a PID vector control for EHVPMSM for an automobile with hybrid technology[J]. Journal of Materials Research and Technology, 2019, 8(1): 54-62.

[28] Mishra A, Makwana J A, Agarwal P, et al. Modeling and implementation of vector control for PM synchronous motor drive[C]//IEEE-international conference on advances in engineering, science and management (ICAESM-2012). IEEE, 2012: 582-585.

[29] Al Harrach M, Dauly G, Seyedeh-Mousavi H, et al. Improving fast ripples recording with model-guided design of microelectrodes[J]. IEEE Transactions on Biomedical Engineering, 2023, 70(8): 2496-2505.

[30] Giordano D, Delle Femine A, Gallo D, et al. Traceability for AC ripple over DC current[J]. IEEE Transactions on Instrumentation and Measurement, 2024, 73: 1-9.

[31] Chen J, Wang Z, Huang J, et al. A configurable dc–dc ripple attenuator module with an active ripple cancellation technique[J]. IEEE Transactions on Power Electronics, 2024, 39(6): 7217-7229.

[32] Su Z, Sun X, Lei G, et al. Augmented continuous-control-set model predictive current control for dual three-phase PMSM drives[J]. IEEE/ASME Transactions on Mechatronics, 2024, 30(3): 2367-2378.